PDMMLA derivatives as a promising cardiovascular metallic stent coating: Physicochemical and biological evaluation

R. Belibel, S. Sali, N. Marinval, A. Garcia-Sanchez, C. Barbaud, H. Hlawaty

Version of Record: https://www.sciencedirect.com/science/article/pii/S0928493120332021
Manuscript_76efbb019f5cb263cdbdefe6657cea95

PDMMLA derivatives as a promising cardiovascular metallic stent coating: physicochemical and biological evaluation

R. Belibel [1], S. Sali [2], N. Marinval [3], A. Garcia-Sanchez [4], C. Barbaud [2]*, H. Hlawaty [3]

[1] KymiaNova, F-92290, Châtenay Malabry, France.

[2] Université Sorbonne Paris Nord, Institut Galilée, Laboratory for Vascular Transitional Science (LVTS), INSERM UMR 1148, F-93430, Villetaneuse, France

[3] Université Sorbonne Paris Nord, SMBH, Laboratory for Vascular Translational Science, INSERM UMR 1148, Groupe Biothérapies et Glycoconjugués, F-93400, Bobigny, France.

[4] Université Sorbonne Paris Nord, Institut Galilée, Laboratoire des Sciences des Procédés et des Matériaux, CNRS UPR 3407, F-93430, Villetaneuse, France.

Keywords

Biodegradable PDMMLAs; stent coating; biocompatibility; biological response; HUVECs; monocytes adhesion.

Abstract

To reduce the risk of intra-stent restenosis and improve hemocompatibility of biomaterials, the therapeutic re-endothelialization is required. Indeed, the behavior of endothelial cells is affected by several factors such as wettability and surface energy of biomaterial in contact with cells and blood. The aim of this study was to evaluate the physicochemical and biological properties of new polymers derived from poly(*(R,S)*-3,3-dimethylmalic acid) (PDMMLA) that will be used as cardiovascular stents coating. In fact, a comprehensive study of the roughness and topography and the thermal and rheological properties of these materials were investigated. Furthermore, this was correlated with the biological response of human vascular endothelial cells (HUVECs) and monocytes (MM6) to these biomaterials. Our results revealed very interesting surface properties of PDMMLAs, excellent thermal and thermo-mechanical properties and a suitable biological response. All these properties can be adjusted by simple chemical modification of the side chain of the studied polymers.

*Corresponding author: E-mail address: barbaud@univ-paris13.fr, Tel.:+33(0)149403357. Fax: +33(0)149403083

1. Introduction

Atherosclerosis which is characterized with artery occlusion is the major etiology of cardiovascular diseases, thereby representing one of the major causes of death and disability in industrialized countries [1]. For treatment of this pathology, the use of metallic endovascular stents has been a revolutionary advance in recent years [2]. Although this progress has been effective in opposing acute elastic recoil of the affected artery, complications observed following stenting procedure have led to in-stent restenosis in 30% of cases within three months of the intervention [3]. This treated artery re-obstruction is the result of several phenomena: vascular endothelial cells (ECs) death, smooth muscle cell (SMC) proliferation and migration from media to neointima, inflammatory cells displacement from blood to vascular wall (monocytes and leucocytes) and the local inflammation due to metal corrosion [3,4]. Therefore, the coating of metallic stent was a promising solution to overcome this problem in order to enhance re-endothelialization, inhibit SMC proliferation and migration and improve interactions between biological environment and material. The re-endothelialization is significantly influenced by endothelial cell attachment, spreading and proliferation which have an important role in evaluating the coating material performance.

During the last decade, several polymeric coatings (non-degradable and biodegradable polymers) have been successfully used for coating a metal stent and thus reduce the risk of in-stent restenosis compared to non-coated stents [5]. These polymers are usually used as drug-eluting supports [6,7]. For this purpose, biodegradable polymers that may be completely metabolized have given the best solution to the long-term effects of durable polymers having then an acute inflammatory response that causes rapid progression of treated artery restenosis [8]. This new generation of drug eluting-stents has remarkably decreased the risk of thrombosis related to the non-coated stents and covered-stent without durable polymers.

Polyesters are the family of biodegradable polymers the most widely used as drug-eluting supports thanks to their high biocompatibility and non-toxicity such as PLA (polylactic acid), PGA (polyglycolic acid) and their copolymer PLGA (polylactic-*co*-glycolic acid) which gave promising results [9]. In contrast, their use as drug-eluting supports is still limited because of their metal-adherence properties and degradation time issues that affected by various factors such as polymer molecular weight or medium pH that influence on the control of drug release kinetics on one hand. On the other hand, the clinical complications associated to late thrombosis, inflammation processes and endothelial healing delayed are observed. These studies are still in clinical trial or in research stage and remain in need of complete or improve [4].

Therefore, elaborating the best biodegradable polymeric coating having at the same time good metal-adherence and mechanical properties required for use as drug eluting-stent, an excellent biocompatibility, a capacity to release a drug in good defined time, accelerate re-endothelialization, minimize the risk of late thrombosis and acute inflammatory reactions is the current challenge of scientific research in cardiovascular biomaterials domain.

Ideally, it would be interesting to study bioactive polyester as an endovascular stent coating, which thanks to its mechanical and chemical surface properties, would release the graft drug in a controlled manner. Therefore, before grafting the drug on the polymer and proceed to the study of its controlled-release, it is necessary to study its physicochemical and mechanical properties, its rates of *in vitro* degradation and its effects on vascular cells behavior without bioactive molecule. In addition, *in vivo* degradation study of PDMMLAs copolymers without drug grafting will be presented in other works. In this study, we study non-drug polyesters derived from poly((*R*,*S*)-3,3-dimethylmalic acid) (PDMMLA) to choose the promising bioactive coating of metallic stents (Fig. 1). The study of PDMMLAs copolymers with drug grafting will be presented in other papers.

Indeed, this polymer is chosen for several reasons. Firstly, it belongs to the *poly(malic acid)* (PMLA) family which is known to present good biocompatibility, non-cytotoxicity *in vitro* and *in vivo*, non-immunogenic properties and stability in the bloodstream [10–16]. Furthermore, in comparison with PLA, PMLA has good affinity to human vascular endothelial cells (HUVECs). It was copolymerized with PLA to improve cellular affinity (attachment, spreading and proliferation) and prevent platelet aggregation [16–19].

Moreover, PDMMLA is an amphiphilic amorphous synthetic biodegradable polymer, unlike to PLA, it can be chemically modified to provide different chemical groups; this may be adapted to modifying hydrophilic/hydrophobic balance and thus changes its degradation rate. It may contain a lateral alkyl group or a functional group such as a chemically modified unsaturated bond, or an ester group, which will be transformed into carboxylic acid group for coupling of sophisticated groups and bioactive molecules. Then, it can have on the lateral chain a drug to release during its degradation; we hypothesize that the grafting of drug could be done either during the synthesis of the monomer or on the polymer after deprotection. In addition, PDMMLA has two methyl groups in the α-position of the ester function, which increases its hydrophobicity and allows control of molecular weight without transfer reactions relative to PMLA [20,21].

Moreover, besides all these properties, its chemical architecture is predefined to provide biocompatible biomaterials giving natural and non-cytotoxic primary hydrolysis products after their complete degradation. It was reported that, the hydrolysis of amorphous PDMMLA gave the corresponding (*R*,*S*)-3,3-dimethylmalic acid [21]. Indeed, diacid (*R*)-3,3-dimethylmalic acid, the final product of hydrolytic degradation of chiral PDMMLA is a natural and non-cytotoxic product that enters in the biosynthetic pathway of pantothenate [22–24]. We further consider that this biodegradable polymer is bioassimilable. In addition, the physicochemical and mechanical properties of this polymer have attracted our attention to evaluate its behavior as coating of metallic endovascular stents.

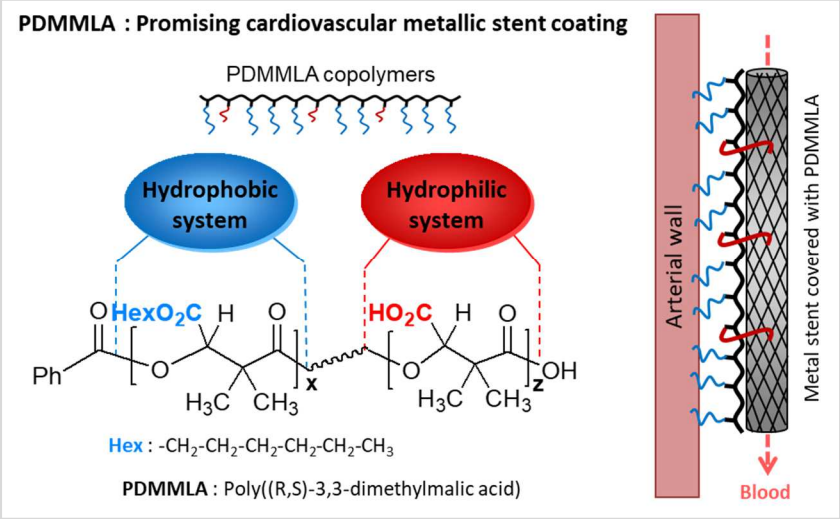

Fig. 1.: Promising metallic stent coating representation.

Our previous works have demonstrated the synthesis of PDMMLA copolymers [21,25]. For this work, we have chosen to synthesize three amphiphilic amorphous statistical copolymers composed of different hydrophilic/hydrophobic proportions of functional groups in their side chains: PDMMLAH$_{10}$-*co*-Hex$_{90}$, PDMMLAH$_{20}$-*co*-Hex$_{80}$ and PDMMLAH$_{30}$-*co*-Hex$_{70}$. The carboxylic acid groups (H) were used for their hydrophilic character while the hexylic groups (Hex) were used for their hydrophobic behaviour [21,25].

The present work is focused on the evaluation of these copolymers for the aimed biomedical application which would consist of favoring re-endothelialization and having better thermo-mechanical properties. Several techniques were carried out for this aim. Differential scanning calorimetry (DSC), rheology, atomic force microscopy (AFM) and scanning electron microscopic (SEM) were used to identify their thermo-mechanical and surface properties. Furthermore, in correlation with these analysis, we are finally designed our study with *in vitro* assessment of the biological response to presence of different copolymers. The biomaterials impact was studied for

HUVEC attachment, adhesion, morphology analysis and lactate dehydrogenase (LDH) proliferation assay. The adhesion of monocytes on PDMMLA films was also performed. Finally, the obtained results with studied PDMMLA copolymers will be compared with those of PLA which is the most used material as stent coating.

2. Experimental procedure

2.1. Polymer synthesis and characterizations

Amorphous PLA (M_n = 20 000 g/mol) was purchased from Sigma Aldrich (France). Anhydrous tetrahydrofuran (THF) was distilled on sodium-benzophenone. In all other cases, the commercially available chemicals were purchased from Sigma Aldrich (France) and employed as received. All reactions, with anhydrous organic solvents were performed under nitrogen atmosphere. Synthetic and amorphous poly((*R*,*S*)-3,3-dimethylmalic acid) (PDMMLAs) were prepared in anhydrous THF solution by Ring Opening Polymerization (ROP) of racemic β-lactones monomers using the previously reported procedure with the tetraethylammonium benzoate as initiator [21,25]. The monomers were synthesized according to the literature procedure as well with different functional groups to bring the acidic hydrophilic and hydrophobic characters for polymers [26] (*Synthesis, Scheme S1 in the ESI*). In this study, three statistical copolymers having different functional groups in their side chains were prepared. They were synthesized with different acidic hydrophilic/hydrophobic percentages (PDMMLAH_{10}-*co*-Hex$_{90}$, PDMMLAH_{20}-*co*-Hex$_{80}$ and PDMMLAH_{30}-*co*-Hex$_{70}$). The carboxylic acidic (H) and hexylic (Hex) functions were used, respectively, to vary this balance. The polymers with 10, 20 and 30% of acidic groups were named as 10/90, 20/80 and 30/70, respectively.

Theoretical molecular weights (M_{nTh}) of different polymers can be determinate by molar ratio of monomer to initiator [M]/[I]. For copolymers, the initiator was used with 10^{-2} equiv per mol of monomer to obtain M_{nTh} ranges between 22 000 and 30 000 g/mol (Table 1). The different polymers were characterized by Infrared (FTIR) spectroscopy analysis, which showed the ester characteristic band of different polyesters around 1751 cm^{-1} and the disappearance of the lactone band around 1838 cm^{-1} of different *β*-lactones monomers (*FTIR spectra, Fig. S1 in the ESI*). FTIR spectra were recorded on AVATAR 370 TF-IR Thermo Nicolet spectrometer using Nicolet OMNI-Sampler ATR Smart Accessory (Ge, DTGS). Absorption bands are given in cm^{-1}. Then, the ^1H and ^{13}C Nuclear Magnetic Resonance (NMR) spectroscopy was used to confirm the chemical structure of all PDMMLAs and the co-monomers relative contents (10, 20 and 30%) of copolymers. This latter percentage was obtained by ^1H NMR using the integration ratio between the peaks which correspond to hexylic and benzylic -CH_2-O- (*^1H NMR spectra, Fig. S2 in the ESI*) [25].

The absolute average molecular weights and molar mass distribution were determined at room temperature by coupling online a high performance size exclusion chromatograph (HPSEC), a multi-angle laser light scattering detector (MALLS), a viscometer and a differential refractive index (dRI) detector. THF, used as carrier, was filtered through a 0.1 µm filter unit (Millipore, Billerica, USA), carefully degassed (DGU-20A3R Shimadzu, Kyoto, Japan), and eluted at a 0.5 mL/min flow rate (LC10Ai Shimadzu, Kyoto, Japan). 100 µL of a 0.2 µm-filtered sample solution (at about 20) were injected with an automatic injector (SIL-20A HT Shimadzu, Kyoto, Japan). The column packing was a polystyrene-divinylbenzene gel. The MALLS photometer, a miniDawn TREOS from Wyatt Technology Inc. (Santa Barbara, CA, USA) was provided with a fused silica cell and a Ga-As laser (λ = 665.8 nm). The whole collected data: light scattering (LS), dRI were analyzed using the Astra v6.0.6 software package. Molar mass was obtained with the Zimm order 1 method. The concentration of each eluted fraction was determined with dRI (RID10A Shimadzu, Kyoto, Japan) according to the measured values of dn/dc (0.05 mL/g) [27]. For all polymers, high molecular weights with a very good molar mass distribution value (Đ) which close to unity was observed. The molecular weight of commercial amorphous PLA was found different than indicated (Table 1).

Table 1. Characteristics of PLA and PDMMLA copolymers.

Samples	Molecular weights (g/mol)				Wettability (°)		Surface free energy (mJ/m^2)		
	M_{nTh}	M_n	M_w	Đ	θ_S	θ_A	γTOT	LW	AB
PLA	20 000	12 800	13 040	1.018	77.28	81.69	49.18	46.01	3.17
10/90	22 860	17 950	18 700	1.041	88.73	102.67	41.21	38.22	3.01
20/80	22 920	17 100	17 400	1.017	85.94	95.29	44.19	36.86	7.32
30/70	22 980	17 510	18 100	1.033	81.10	94,31	47.5	35.79	11.59

2.2. Preparation of polymer films

To obtain polymer films, the PDMMLAs were dissolved in acetone and PLA in chloroform. Firstly, for AFM measurements, the polymer solution was then deposited on glass slides. After the evaporation of solvent at room temperature, glass slides were dried at 37°C overnight in a vacuum oven. Secondly, for cell culture, the polymer solution was coated in glass crystallizers having the same diameter than 24-well to carry out proliferation assays and in glass LabTek for spreading and adhesion tests. They were sterilized in the ultraviolet light for 1h prior to cell culture. Before cell seeding, the polymer films were incubated with pretreatment media for 2h (*this time was developed during a previous work in our laboratory*).

2.3. Physicochemical and mechanical properties

2.3.1. Atomic Force Microscopy (AFM)

AFM was used to obtain topographic images of surface samples. The AFM machine was a nanoscope 5 (Bruker-Nano) and the cantilever was a Veeco tip silicon probe with aluminum reflex coating (resonant frequency: 300 kHz) and with a constant force of 40 N/m. Imaging was performed in the air, at room temperature, and using the tapping mode. Surface morphology and roughness parameters were determined by the AFM software program. The (10 µm x 10 µm) 2D images of topography were obtained with a resolution of 256_256 pixels. Surface roughness and topography parameters (*Ra*, *RMS*, *RSk* and *RKu*) were then evaluated from 10 µm x 10 µm (100 μm^2), 5 µm x 5 µm (25 μm^2) and 2 µm x 2 µm (4 μm^2) images.

2.3.2. Thermal analysis

All glass transition (T_g) temperatures of different polymers were obtained using Differential Scanning Calorimetry (DSC). It was measured on a SDT Q600 analyzer (TA instrument, France). In a typical run, polymers were first put in the furnace and heated from -60°C to 200°C by means of a temperature ramp of 10°C/min. This operation was repeated twice. T_g was determined from the inclination point of the second heating curve. Thermogravimetric analysis data were obtained with a TGA Q50 at a heating rate of 10°C/min under N_2 atmosphere.

2.3.3. Rheological analysis

Rheological measurements were performed using 40 mm diameter parallel plate geometry. The variation of the storage modulus (G'), loss modulus (G'') and phase angle δ were measured as a function of frequency at 37°C. An oscillatory stress at frequencies ranged between 0.2 and 2 Hz (interval including the value of the average heart rate of 1 Hz) and an amplitude of 1Pa. For each point, the sample was equilibrated for 3s ("conditioning time") and each value is an average taken, subsequently, over a period of 3s ("sampling time").

2.4. Biological properties

2.4.1. HUVECs cell culture

Cell culture of *Human Umbilical Vein Endothelial Cells* (HUVEC, N° CRL- 1730, ATCC, LGC Molsheim, France) was performed in Endothelial Cell Basal Media 2 (ECBM2, PromoCell, Germany) supplemented with 10% fetal bovine serum, epidermal growth factor (EGF, 5.0 ng/mL), hydrocortisone (0.2 µg/mL), VEGF (0.5 ng/mL), basic fibroblast growth factor (bFGF, 10 ng/mL), insulin like growth factor (R3IGF-1, 20 ng/mL), ascorbic acid (1 µg/mL), heparin (22.5 µg/mL), antibiotics (1% penicillin-streptomycin, from PAA Laboratories, Pasching, Austria). HUVECs were

seeded using ECBM2 complete media and incubated at 37°C in 5% CO_2 for 24h to obtain adherent and proliferating cells. Cells were divided 2 times per week at a sub cultivation ratio of 1:3.

2.4.2. *Spreading test of HUVEC on polymer films*

Spreading of HUVEC was performed on polymer films using 8000 cells/well in coated glass 8-well LabTek in order to analyze changes in individual cell shape and size. After 2h of spreading, the cell media was removed and cells were fixed using PFA 1% and washed by PBS (1X); followed by permeabilization using 0.05% of Triton X- 100 solution (Sigma-Aldrich, France). Cytoskeleton (F-actin) and nucleus were stained subsequently with Alexa Fluor 546 phalloidin (dilution 1/200, Invitrogen, France) and DAPI (dilution 1/1000, Invitrogen, France); and observed with a fluorescence microscope (Zeiss Axiophot, Carl Zeiss, France). Cells were photographed using digital camera fixed on top of the fluorescence microscope (Nikon COOL PIX 8400, Japan). Then the areas (expressed in μm^2) enclosed by each trace were measured using Scion Image software (Scion Corporation) with a minimum of 100 cells counted over 3 different samples for each scaffold type. This was repeated 4 times on different cell passage on different days (n = 4) occupying the same duration for incubation (2h).

2.4.3. HUVEC cells morphology analysis on polymer films

Cellular morphology of different surface films was visualized using *phase contrast microscopy* (Zeiss Axiophot, Carl Zeiss France). HUVEC cells were cultured as described in the "cell culture" section. Cells were incubated on the coated glass-crystallizer with polymers for 1 day, 2 days, 3 days, 4 days and 5 days. Cells were photographed using digital camera fixed on top of the microscopy (Nikon COOL PIX 8400, Japan). For the same surface, 3 different samples were used for each time and repeated 3 times on different passage number on different days (n = 3) occupying the same duration for incubation.

2.4.4. In vitro HUVECs adhesion

For HUVEC adhesion test, after the pretreatment of surfaces with different polymers, 3000 cells/well were deposed in polymers-coated glass 16-well LabTek. The positive control was used in the same conditions without any polymer-coated surface. After 10 min of incubation at 37°C and 5% CO_2, culture media were removed and cells were washed twice with PBS (1X). Then, adhered cells were counted manually using *phase contrast microscopy* in each well and their percentage was normalized to cells number at the beginning of study of cell adhesion. The adhesion test was repeated 3 times (n = 3) in the same conditions.

2.4.5. Monocytes adhesion

The Mono Mac 6 (MM6) human monocytes were deposited in suspension in the culture media at a density of 40 000 cells/well (polymers-coated glass 16-well LabTek) after the pretreatment of different polymer surfaces. The positive control was used in the same conditions without any polymer-coated surface. After 10 min of incubation at 37°C and 5% CO_2, culture media were removed and cells were washed twice with PBS (1X). Then, adhered cells were counted manually using *phase contrast microscopy* in each well. Their percentage was normalized to cells number at the beginning of study. The adhesion test was repeated 3 times (n = 3). Three samples of each polymer film surface were used for each adhesion time and repeated 3 times on different passage number on different days (n = 3) occupying the same duration for incubation.

2.4.6. Proliferation of HUVEC cells on polymer films

The HUVEC proliferation was determined after 24h, 48h and 72h of incubation after initial cell seeding on the different polymer films with the cell culture media. HUVEC cells were cultured as described in the "cell culture" section. Three samples of each polymer film surface were used for each proliferation time and repeated 3 times on different passage number on different days (n = 3) occupying the same duration for incubation. The percentage of cytotoxicity was determined by enzymatic activity measurement of LDH in the HUVEC-conditioned medium using a colorimetric LDH assay (CytoTox 96, Promega, Madison, USA) according to the manufacturer's protocol. Lysis Solution is used to generate a Maximum LDH Release Control. The absorbance of LDH was measured at 490 nm. The average values of the culture medium background were subtracted from all values of experimental wells. Then, the percentage of cytotoxicity was computed as: *Percent cytotoxicity = 100 × (Experimental LDH Release/Maximum LDH Release).*

2.5. Stent-coating

Stainless steel stents were used as coating platform. For removing any dirt or fibers adhering to metallic stents, they were sonicated in acetone, ethanol, 2-propanol and water in sequence. Each step was repeated 3 times for 15 min. The stent coating was performed via immersion of the stent in a solution of 40 g/L of polymer in acetone which was filtered through 0.2 µm syringe filters. The solvent was evaporated at room temperature overnight using the tubes rotator for obtaining a homogeneous coating. Then, coated stents were deployed by expandable balloon catheters. The deployed stents coating was characterized by Scanning Electron Microscopic (SEM) which was carried out by means of a Raith PIONEER System.

2.6. Statistical Analysis

All data are expressed as mean ±S.D. (Standard Deviation) unless indicated otherwise and analyzed using one-way analysis of variance (ANOVA). A difference of $p < 0.05$ was considered significant.

3. Results and discussion

3.1. Physicochemical properties

This section demonstrates the study of surface and thermo-mechanical properties of polymers. The polymer-based stent coating must have, in addition to its good surface properties, good thermo-mechanical properties (glass transition temperature (T_g), decomposition temperature (T_d) and rheological properties). Indeed, T_g affects the mobility and stiffness of the polymer chain. Therefore, the mechanical (viscoelastic) behavior of the polymers is strongly dependent on the T_g value. At atmospheric temperature, the material properties can significantly vary in comparison with its performance *in vivo* where it must withstand a saline and corrosive environment at 37°C. Furthermore, the interactions between implant and biological environment are strongly influenced by the roughness and topography of the implant surface. Indeed, non-homogeneous and asymmetric surface with high roughness can orient the spreading and migration of cells and induce corrosion of biomaterial surface.

3.1.1. Atomic Force Microscopy (AFM)

Atomic force microscopy analysis (AFM) was used to investigate the topography and roughness of the surface polymers film and to finally verify the possible correlation between the surface morphology and cell behavior.

Figure 2 showed the 3D AFM images of the top surface of the different samples: glass without polymer (control) and the thin films of PLA, 10/90, 20/80 and 30/70 deposited on the glass coverslips from solutions within the same scan areas of 10 µm x10 µm, while presenting the cross-sectional profile as a function of vertical distance for each analyzed surface. Hence, for compare and obtain the detailed view of the investigated samples topography, several parameters were studied in this chapter: root mean squared roughness (*RMS*), skewness (*RSk*) and kurtosis (*RKu*).

- *Height Parameters*

This study revealed that the three copolymers roughness is very low, and their 3D images showed more favorable surface parameters in comparison with those of the bare glass and the PLA. Figure 2 showed Cross-sectional profiles as a function of vertical distance that revealed the difference between the five surfaces. This average height profile difference was due to either the difference of surface (glass/polymer), to the difference of the main chain of polymer (PLA/PDMMLA) or to the difference in side-chain composition indicating, this time, the three copolymers. The cross-section profiles of the surface structure of polymer films appeared not similar to the glass structure. It shows in sequence that the peak intensity increased with the increase of the amount of COOH in the

side chain of the three copolymers which is explained by the increase in the surface chemical heterogeneity.

The 10/90 copolymer which has the lowest COOH content (10%) appeared almost linear with very small and not-sharp peaks throughout the scan, having very low heights making the smoother surface. On the contrary, the 30/70 copolymer which has 30% of COOH side-chain, shows the tallest height profile and the 20/80 copolymer which provides the average content of COOH, presents therefore an average profile of the cross-section. However, the PLA sample shows unusual intense and large peaks. The reason is not clear but in accordance with the literature [28,29].

RMS values revealed also this significant difference between the samples surfaces. This difference was translated (*RMS values, Fig. S3 in the ESI*) demonstrating that the surfaces had a slightly higher profile after the addition of a certain amount of COOH in the copolymers side-chain and *RMS* value was increased with increasing of COOH content. A correlation is also observed for glass and PLA having higher *RMS* values. In fact, these surfaces presented low values to very low for copolymers. They remained smooth without exceeding the *RMS* value of 0.1 µm.

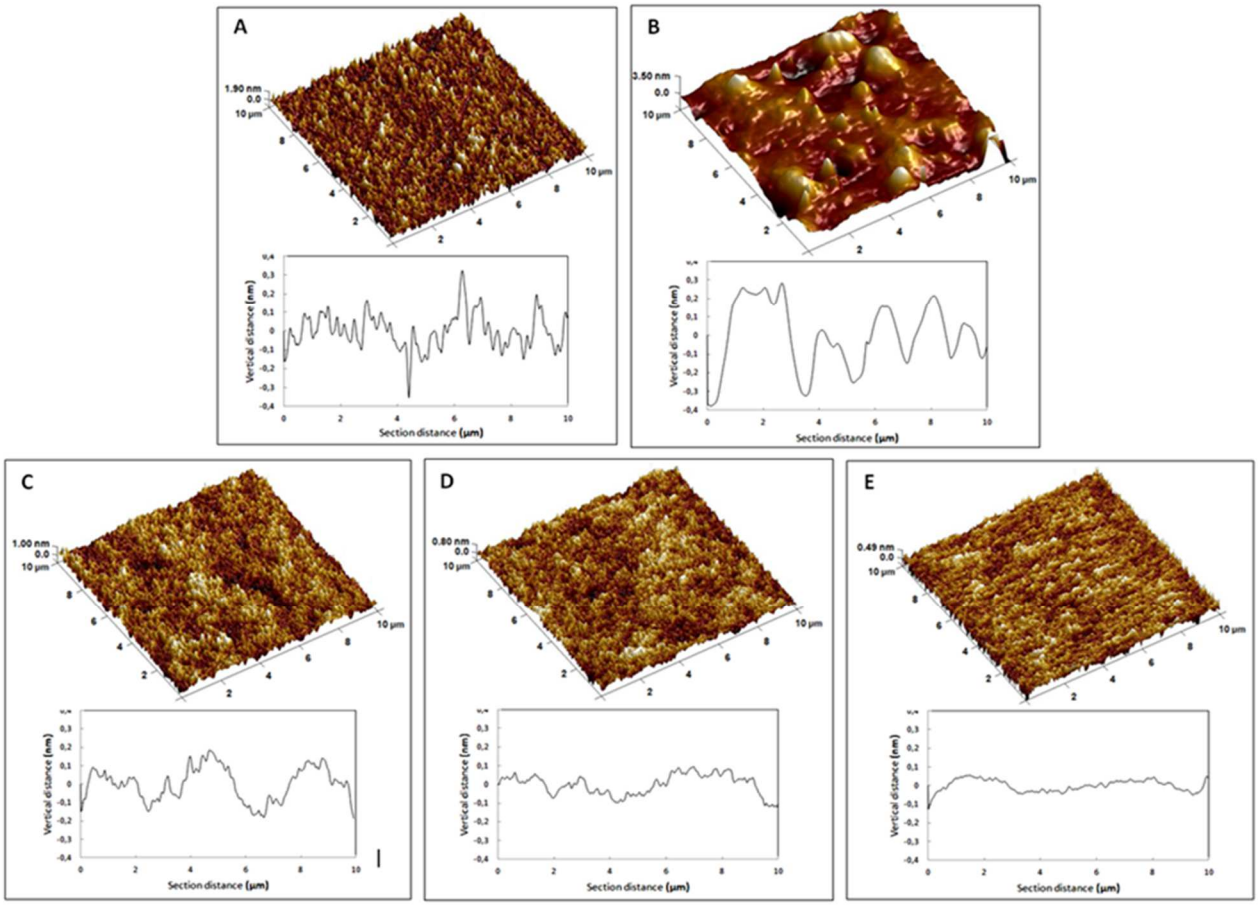

Fig. 2. Study of height and functional parameters of different samples. 3D AFM images and Cross-sectional profiles of **(A)** Glass, **(B)** PLA, **(C)** 30/70, **(D)** 20/80 and **(E)** 10/90.

❖ *Functional or Statistical Parameters*

RMS characterized the height of irregularities of profile at different paces but not the form of the surface roughness. It was thus not sufficient to fully characterize the flattening of the materials surface. Indeed, several forms presenting different appearance profile can have very similar *RMS* values but they may have a completely different behaviour in friction and wear.

To reinforce the previous conclusion and give more information about the surface of different samples and so characterize the tribological profile in respect of the physiological environment, Skewness (*RSk*) and Kurtosis (*RKu*) were studied in this work. Indeed, the *RSk* average values were found very close to zero for the three copolymers, so that the three films presented a symmetrical surface compared to glass and PLA results. The 20/80 and 30/70 were the more planar films with a negative value close to zero. Besides, *RKu* values suggested that all samples gave almost similar average values which were close to 3, except PLA (*RSk values, Fig. S3 in the ESI*). Therefore, varying the amount of COOH in the side-chain from 10% to 30% had almost no influence on flattening of copolymers films indicating an intimate homogeneous mixing of the copolymers hydrophobic and hydrophilic compositions. It is observed that *RSk* and *RKu* parameters vary simultaneously.

Therefore, the three copolymers presented significant differences ($P < 0.01$) (*RMS values, Fig. S3 in the ESI*) observed between the different results obtained with all parameters studied in this chapter. The appearance of the three copolymers films in 3D images was almost similar. Indeed, only one homogeneous phase is observed. The two heterogeneous side-chains and the deposits dispersion of the different surfaces of copolymers were not visible. This indicated that the three copolymers showed a uniform and smoother profile with a planar and symmetric surface. It represents an opportunity to be an innovative and favorable coating candidate for metallic endovascular stents.

In order to prove this homogeneity and uniformity throughout surface of the copolymers film in comparison with PLA film, several scans were made at different places within the same scan areas for each sample: 10x10 μm^2, 5x5 μm^2 and 2x2 μm^2 followed by a statistical study determining thus the standard deviation on the different parameters for each surface. All histograms of *RMS*, *RSk* and *RKu* results obtained on these different areas scans where no significant differences in the three groups (10x10 μm^2, 5x5 μm^2 and 2x2 μm^2) for copolymers and glass were observed (*Fig. S3 in the ESI*).

This reproducibility of the different results was obtained with very small standard deviations for each parameter. In contrast, a significant difference ($P < 0.05$) was observed between PLA groups for each parameter which revealed the presence of plan and symmetric areas simultaneously with rough and asymmetric regions irregularly dispersed. 2D AFM images of PLA and 10/90 copolymer confirmed this difference. Note that for the 10/90, whatever the area scan (10x10, 5x5 or 2x2 μm^2), the surface was homogeneous and uniform, unlike the PLA which represented simultaneously very smooth zones (2x2 μm^2) and rough regions (10x10 and 5x5 μm^2) (*Fig. S4 in the ESI*).

In conclusion, this study demonstrated that PDMMLAs have a smooth and flat surface with negligible roughness. Thus, these results can improve the topographic properties of the surface of metallic stent which generally has a high roughness. This is very encouraging to continue the thermo-mechanical testing of these polymer's films.

3.1.2. Thermal properties

According to a number of studies in literature, the flexibility of the polymer chains, steric hindrance, intermolecular attractions, forces and other steric effects were the main parameters that influencing T_g values [30]. In this study, Differential scanning calorimetry analysis (DSC) was carried out in order to obtain the different values of T_g of amphiphilic copolymers (10/90, 20/80 and 30/70).

As mentioned above, the three copolymers studied here contain in the side chains a mixture of carboxylic acid group and hexyl group. Characteristically, the PDMMLAH homopolymer (100/0) has a higher T_g reached a maximum at +68°C [25]. Owing to the mobility restriction of the chains, this phenomenon was explained by the large number of hydrogen bonds formed by interchain interactions. In contrast, the presence of hexyl group in the side chain of PDMMLAHex homopolymer (0/100) makes the movement of polymers chains more flexible and decreases the T_g to a low value reached a minimum of -15°C [25]. In this case, the homopolymer appeared as a soft and viscous system which was also apparent from rheological studies discussed later.

As a result, by decreasing the -COOH content and increasing the -CO_2Hex content respectively in the structure of the three synthesized copolymers, an increase in the flexibility and a decrease in the viscosity of these copolymers were observed. In addition, the variation of the two chemical groups in their structure allowed to determine by DSC values of T_g in adequacy with the biomedical application studied. For our application, PDMMLAs will be used in physiological systems. T_g of polymer-coatings should preferably be less than the physiological temperature (37°C) which could

lead to mobility of polymer chains past one another. Higher temperature acts to destabilize a viscoelastic network and subsequently change the release characteristics (Fig. 3a).

In addition, any melting or crystallization events were observed, indicating that all of the copolymers were amorphous. All of the materials were statistical confirmed by the single T_g value observed for each of them. The point of inflection of DSC scans determined the T_g that was obtained with a significant difference for the three samples. Considering that the T_g in our case varies from -15°C to +70°C, the T_g values of the three copolymers were logically found intermediate between these two values: -14°C, +8°C and +20°C corresponding to 10/90, 20/80 and 30/70 copolymers.

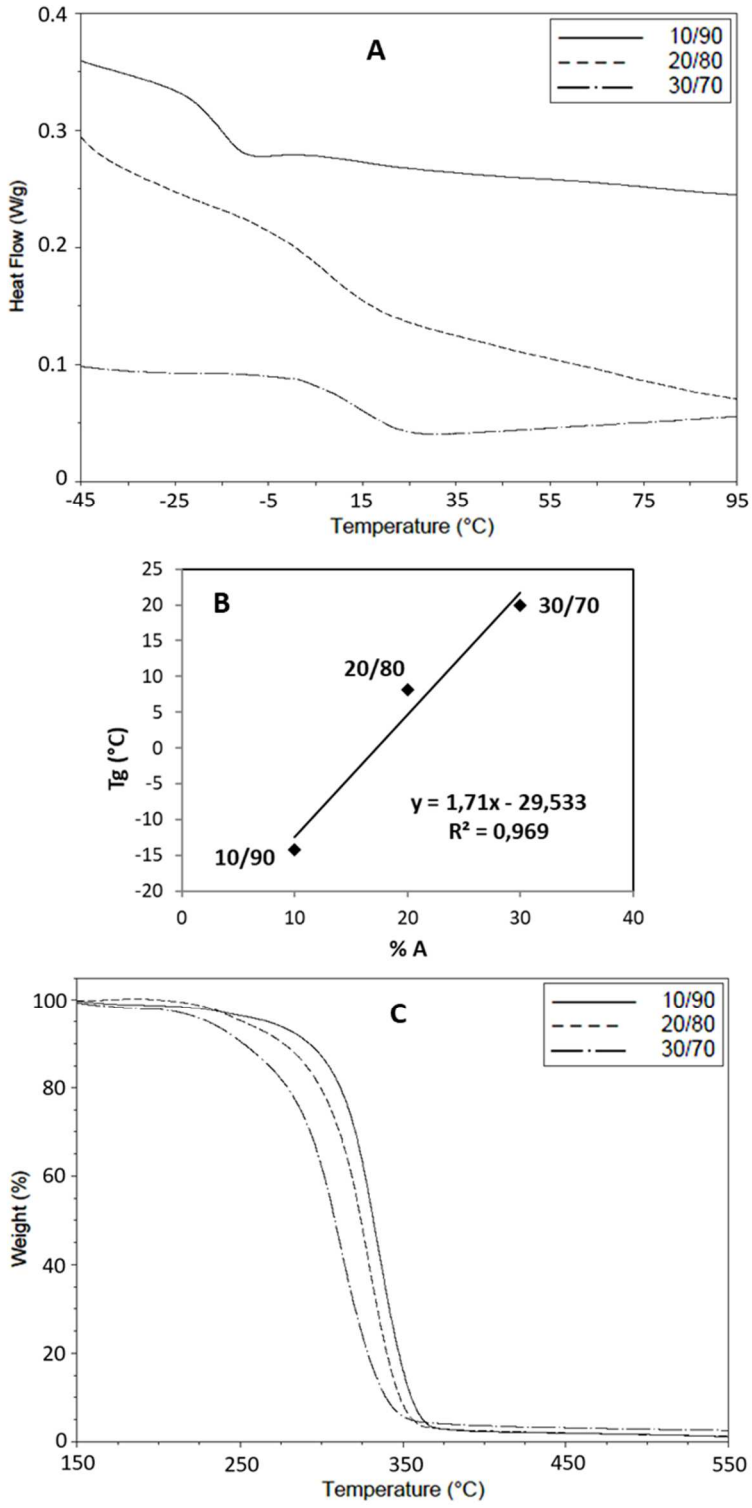

Fig. 3. Thermal properties of PDMMLA copolymers (10/90, 20/80 and 30/70): **(A)** 2nd DSC heating scans, **(B)** linear relation between polymers compositions (%A) and their T_g values and **(C)** TGA curves.

These results show that T_g values of three copolymers presented linearity as a function on their compositions (percentage of acidic groups %A) with $R^2 = 0.969$ which confirmed the ideal mixing of the copolymers system (Fig. 3b). Finally, these different values have not reached the

physiological temperature as compared to PLA which had a higher T_g (about 63°C) having thus less ductility and softness.

Thermal stability of PDMMLA polymers was studied in this work, Thermogravimetric analysis (TGA) was performed in a range of 0 and 700° (Fig. 3c). It showed the thermogram curves of different copolymers (10/90, 20/80 and 30/70). They exhibited an initial thermal degradation at about 160°C. However, their T_d was found, respectively, at 331, 323 and 307°C. This indicated that PDMMLA copolymers have good thermal properties and great stability. According to literature, PLA exhibits an onset and maximum degradation temperatures of 211.9 °C and 324.8 °C, respectively [31].

3.1.3. Rheological properties

The rheological study was investigated in order to determinate the viscoelastic properties of the polymers at 37°C. Figure 4 showed the obtained data of elastic modulus (G'), loss modulus (G'') and (tan δ) of the different samples at a deformation frequency of 1Hz and 37°C. In addition, the effect of the ratio of functional groups (hydrophilic/hydrophobic) on the viscoelastic behavior of PDMMLA copolymers was also studied.

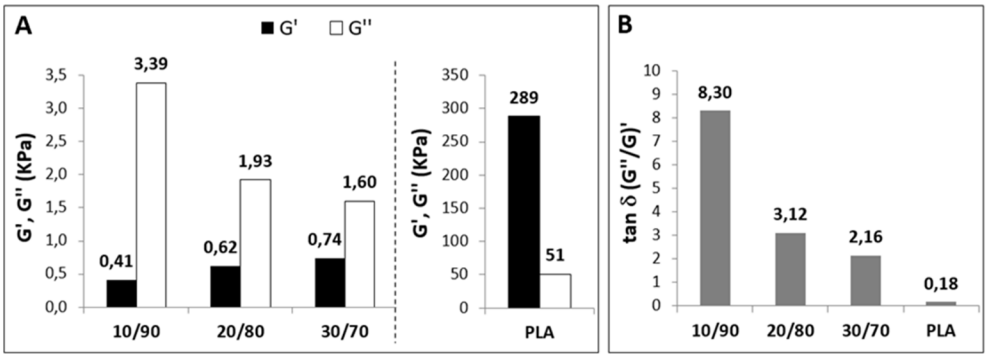

Fig. 4. Rheological properties of PDMMLA copolymers (10/90, 20/80 and 30/70) and PLA as a function of their chemical composition at 37°C and 1Hz: **(A)** storage modulus (G') and loss modulus (G'') and **(B)** tan δ.

Indeed, it was found that the loss modulus (G'') decreased with an increase of carboxylic acid groups in polymer chains while elastic modulus (G') increased slightly. Also, (tan δ) remarkably decreased with the increase of acidic functions in the chain of the different polymers 10/90 (tan δ = 8.3), 20/80 (tan δ = 3.12) and 30/70 (tan δ = 2.16). Therefore, the percentage of hydrophilic groups in the side chain of polymers affected not only their thermal behavior but also their viscoelastic properties. Herein, it was found that the three copolymers had both a viscous and elastic behavior and that the viscous character was predominant. In contrast, PLA exhibited very high value (289

KPa) of elastic modulus (G') which indicated the stiffness of a viscoelastic material as compared to PDMMLA polymers. It had very low loss tangent (tan δ) value (0.18). Therefore, PLA had more elastic character than viscous.

These results were in accord with DSC results which showed that the rigidity of the polymer chains decreased with the decrease of the carboxylic acidic groups. In summary, as a comparison between the PDMMLAs amorphous copolymers, 10/90 was the most viscous and 30/70 the most elastic. 20/80 owned the average values of all parameters. This means that they have viscoelastic character and flexible chains which can be modulated with varying hydrophilic/hydrophobic balance whereas PLA has high rigidity and ductility.

In this part, we demonstrated that PDMMLAs have a viscoelastic character and T_g values which have not reached the physiological temperature. These parameters were influenced by the chemical composition of the polymers. These results are particularly important for our study. They favor the use of PDMMLAs as coating of metallic stents after completing them by the wettability and surface free energy study. In addition, PDMMLAs have good thermal stability, which broadens its areas of application [25].

3.2. Biocompatibility

Biocompatibility, biodegradability, mechanical properties, and drug-loading capacity are the general considerations of a selected polymer as stent-coating for eluting drugs. Indeed, the surface properties (surface texture, wettability, charge and energy) of the polymer which covers the stent are the main factors that affect the biological response (immediate and long-term response) between the stent, the vascular wall and blood. According to literature, the surface energy is the most important factor in determining the thrombogenicity in blood. The affinity of the polymer surface with water increases with increasing surface energy and therefore with the increasing of thrombogenicity in the blood [32]. It was thus the purpose of other papers to discuss the wettability in static and in dynamic conditions and the surface free energy and its components. An in-depth work which studied in details the different parameters of wettability and surface free energy and its components of different copolymers was exposed in other paper [25,33]. The main obtained results were presented in table 1 for the all polymers (static contact angle (θ_S), dynamic advancing contact angle at cycle 1 (θ_A), surface free energy value (γTOT), surfaces dispersive (γLW) and acid-base component (γAB)).

Thus, PDMMLAs have good wettability which can be adjusted by a simple functionalization of their side chain. This is another encouraging point to avoid the hydrophobicity of PLA, which

requires its copolymerization with other polymers in order to chemically modify and/or modulate its wettability properties. Next, surface energy is the most important factor in cell attachment and spreading. In this study, we demonstrated that PDMMLAs copolymers have low surface energies.

In addition, the hydrolysis rate of PLA and PDMMLA copolymers was studied in a six-month period in physiological conditions [34]. Indeed, PLA was slowly degraded over time with a molecular weight loss of 26% after 6 months. However, the degradation time of all PDMMLA copolyesters were affected with the nature of the side chain of PDMMLA. In a logical order, the loss of molecular weight increased with the increase of carboxylic acid groups (31, 59 and 86% after 6 months for 10/90, 20/80 and 30/70, respectively).

These results were very encouraging for studying for the first time the biocompatibility of PDMMLA polymers.

3.2.1. HUVEC attachment assays on polymer-based films

Endothelial cells adhered to the surface and spread in optimal conditions. In order to determinate the best pretreatment conditions for HUVEC adhesion, their attachment on the surface coated with each polymer films, was carried out after preincubation with three culture media containing different fetal calf serum (FCS) percentages (0%, 12% and 100%) for 2h. Cell assessment and morphology were observed by phase contrast microscopy during 2h after cell seeding on the polymeric surface.

Figure 5 showed the results with 30/70 films in different conditions. It was found that the adhesion and spreading of cells increased with the increase of FCS concentration. Indeed, the cells changed their form from a spherical (black arrows) to a well spread and flat shape (dotted red circle, Fig. 5). In conclusion, the aim of this test was the determination of the best biopolymer-based films conditions for the cell culture. The preincubation of polymer surfaces with 100% of FCS for 2h prior to cell culture was chosen for all other analysis in this work.

Similar results were obtained with the two other films composed by the copolymers 10/90 and 20/80.

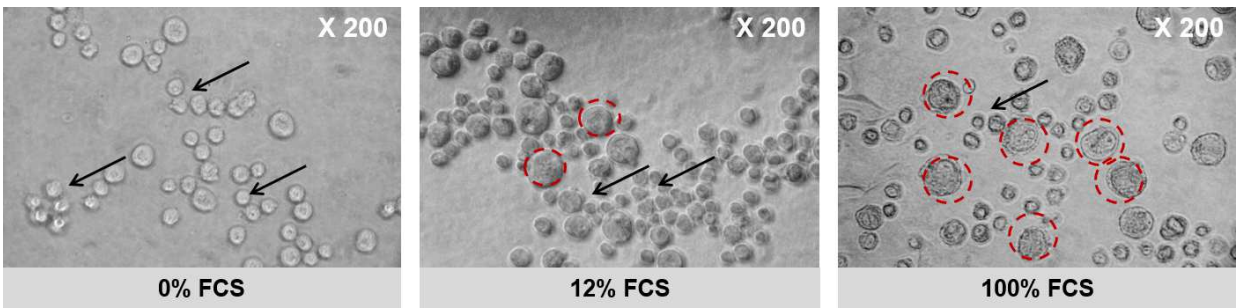

Fig. 5. HUVEC (spherical (black arrows) and well spread and flat shape (dotted red circle)) spreading analysis by phase contrast microscopy after 2h of cell incubation on 30/70 polymer film which was preincubated with FCS for 2h (x200 magnification).

3.2.2. HUVEC spreading analysis on polymer-based films

The cell spreading assay was performed in the presence of different PDMMLA films, to evaluate the morphology and the changes of the cytoskeletal assembly in HUVEC cells. Figure 6 presents the results of cell spreading, morphology and actin cytoskeleton organization after 2h of cell culture on different surfaces analyzed by phase contrast microscopy and fluorescence microscopy.

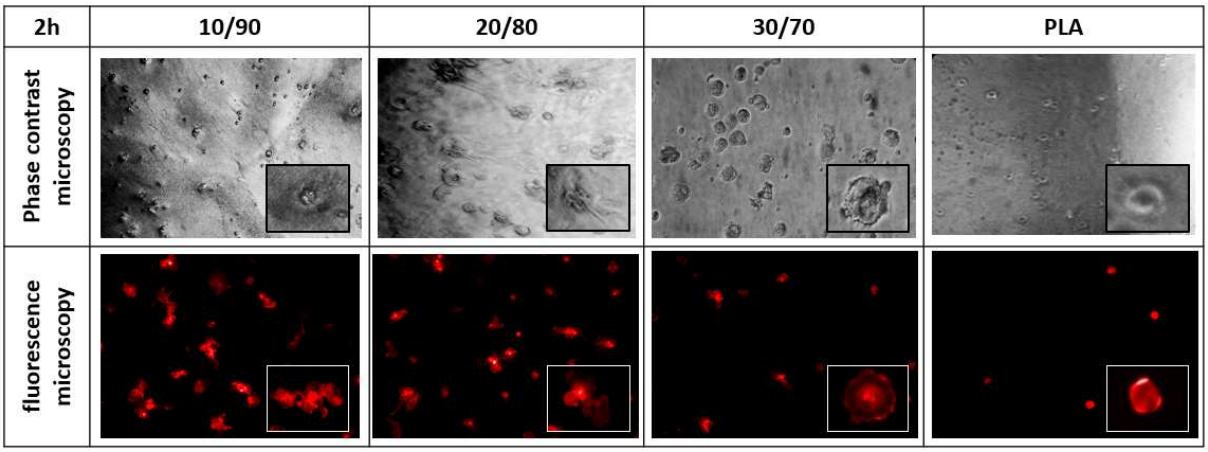

Fig. 6. HUVEC spreading analysis after 2h of cell incubation on 10/90, 20/80 and 30/70 polymer-based films by phase contrast microscopy (upper panel, x200 magnification, high view insert) and fluorescence microscopy (lower panel, x100 magnification, high view insert).

These results showed that the HUVECs spreading in the presence of 10/90 polymer was found more pronounced as compared to the other PDMMLA surfaces. It presented the most hydrophobic surface. In the case of PLA, cells had spherical form and they were not spread.

In addition, the area of HUVEC cells was measured after 2h of cell culture. Figure 7 illustrated the results of the area as a function of polymer surfaces. These results confirmed those observed in Figure 6. The cell spreading decreased with the increase of hydrophilic groups in the PPDMMLAs chains. PLA surface did not permit the optimal cell spreading and lead to the high decrease of cell area.

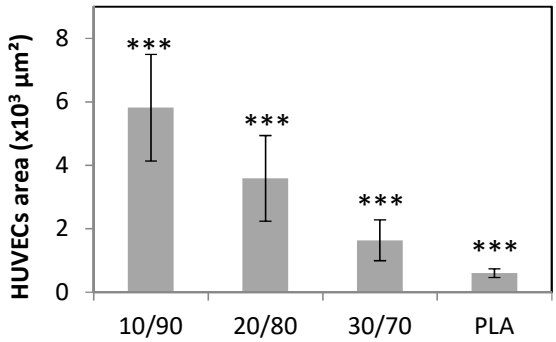

Fig. 7. HUVEC area after 2h of cell culture on different polymer films (10/90, 20/80, 30/70 and PLA). *** $P < 0.0001$.

3.2.3. HUVEC morphology analysis on polymer-based films

The surface of the polymer coating is defined by its external part which is in direct contact with blood. The cells adhesion, morphology and proliferation involved in the interaction of biomaterial with body tissue are generally modulated by its chemical composition in particular by varying their hydrophilic/hydrophobic ratio. The control of the chemical composition of the material allows the modulation of their adsorption [35]. The HUVEC cells have a low affinity for hydrophobic or hydrophilic surfaces. They generally attach to surfaces with a mean value of contact angle (adequate hydrophilic/hydrophobic balance) (*Fig. S5 in the ESI*). According to the literature, the polymers used as synthetic matrices for the coating of stents and the release of drugs are not perfect solutions [6,7]. They have a limited diversity of their structures and adverse reactions can be caused by these polymers [4]. Moreover, the COOH functions of PDMMLAs play an important role in the adhesion of proteins and other components of extracellular matrix thanks to the ionic and hydrogen interactions with the biological medium.

This study was performed in the order to choose the copolymer appropriate. Results showed that the HUVEC cell were well spred on the 30/70 polymers up to day 5 of cell culture, however the 20/80 and 10/90 did not permit good cell attachement and growth (Fig. 8). In addition, in presence of 20/80, HUVEC could not be homogeneously distributed on the whole polymer surface, but they were agregated and formed the small sphere-like 3 dimentinal cell culture from day 3 to 5. In 10/90 culture condition, HUVEC were agregated forming the sphere-like 3 dimentinal cell culture and the polymer monolayer was totally distroyed at day 5. In conclusion, 30/70 had the best properties to favorite HUVECs adhesion.

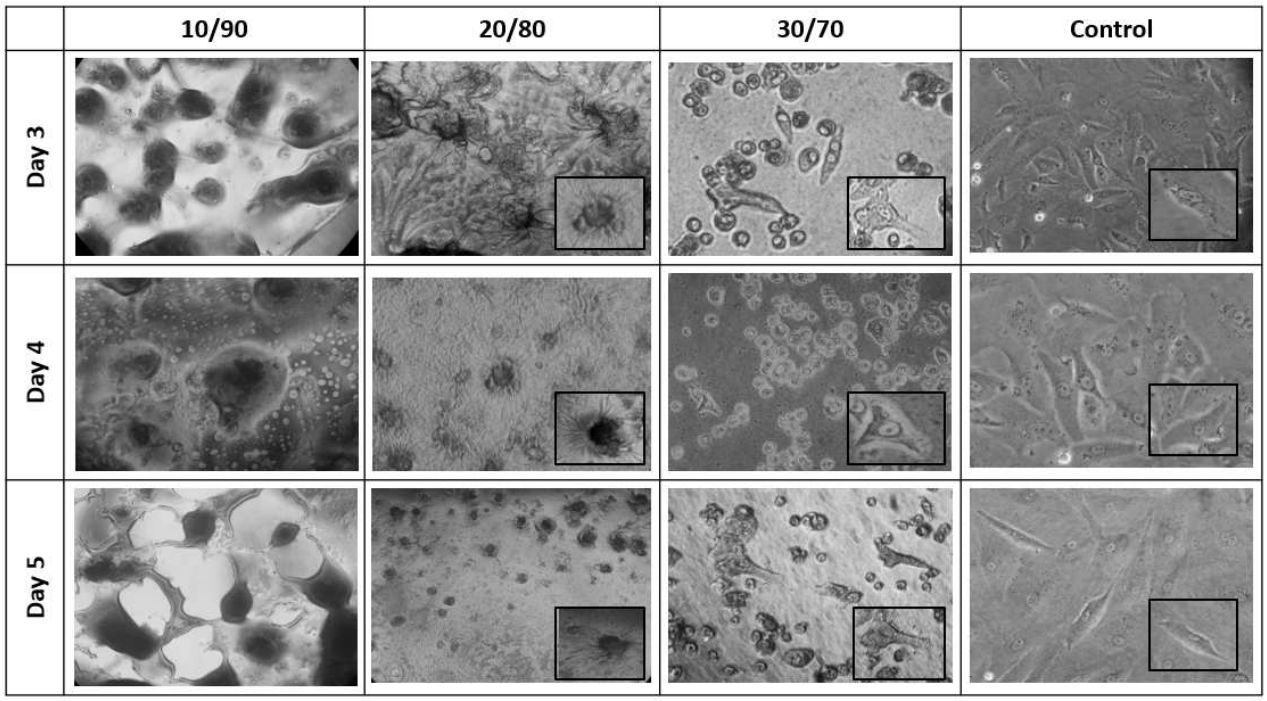

Fig. 8. HUVEC morphology analyzed by phase contrast microscopy on different polymer films (10/90, 20/80, 30/70) and control at 3, 4 and 5 day of cell culture (x200 magnification).

3.2.4. HUVEC adhesion analysis on polymer-based films

In vitro cell adhesion assay was performed to evaluate the HUVEC attachment on different polymer-based films for 10 min (Fig. 9). Consequently, it was found that the 10/90 coated film was the densest surface which reached almost 50% after only 10 min of incubation and so exceeded the control surface. However, the cell adhesion decreased with the decrease of hydrophilic ratio in the chain PDMMLA polymers. The 20/80 and 30/70 coating led to the same percentage of cell adhesion whereas PLA had the smallest percentage. This indicated that 10/90 was the most efficient polymer-based film to favorite HUVEC adhesion.

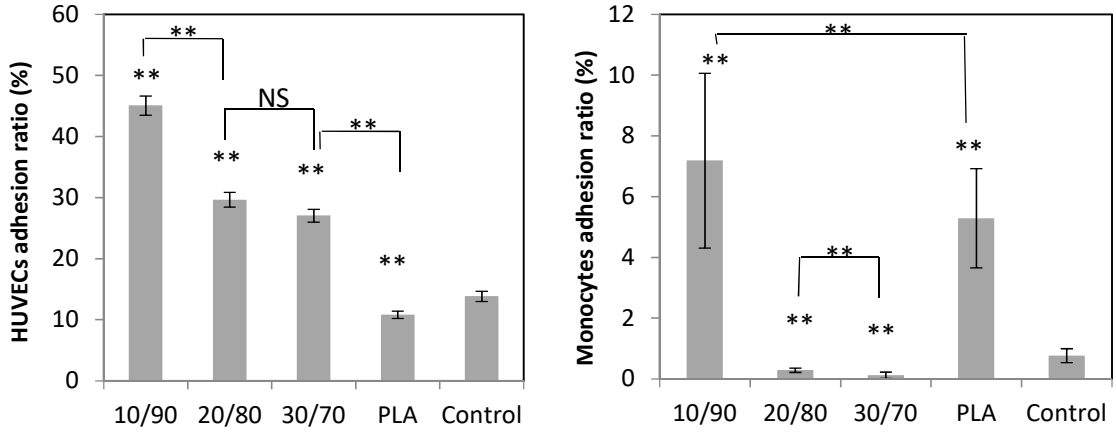

Fig. 9. Adhesion percentage of (a) HUVECs and (b) monocytes on the polymer films and control (without coated polymer). ** $P < 0.0001$, NS (No Signeficant) $P > 0.05$, n=7.

3.2.5. Monocytes adhesion analysis on polymer-based films

After the stent implantation in the artery, the monocytes may be activated at the alteration site. This means that, the polymer-based stent coating should not favor their adhesion on the recovered stent surface. Thus, the adhesion of monocytes MM6 was investigated in this work within 10 min of incubation. Figure 9 illustrated that the 10/90 was also the densest surface with the PLA while 20/80, 30/70 and control exhibited a lower monocytes adhesion. The 30/70 and 20/80 films layers were the most suitable surface to decrease monocytes adhesion.

3.2.6. HUVEC proliferation and viability analysis on polymer-based films

The proliferation assay was performed on the different surface films (10/90, 20/80, 30/70 and PLA). HUVEC cultured on plastic support (without polymer coating) were used as control and the maximum of LDH release was used as positive control. The supernatant from cell culture after 1, 2 and 3 days of incubation was analyzed by LDH assays according to the manufacturer's instructions. The LDH activity is proportional to the amount of cell death. As result, higher LDH activity indicated more cell damage (Fig. 10).

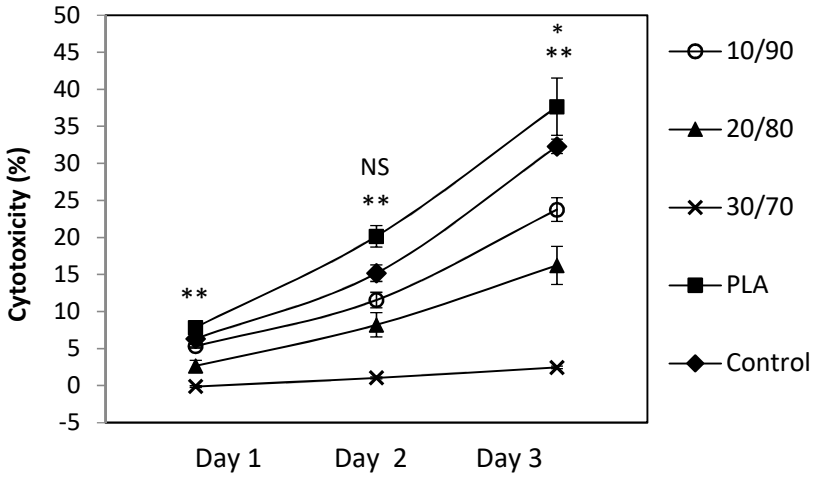

Fig. 10. Assessment of cell viability of different substratum (10/90, 20/80, 30/70, PLA and control) using LDH assay as a function of HUVEC incubation time (1, 2 and 3 days). Cytotoxicity was determined from the formula described in the materials and methods section. Significant difference between the 3 days for each sample (** $P < 0.0001$, n=9). Significant difference between samples for the same day (** $P < 0.0001$, * $P < 0.01$, n=9 (between PLA and control) and NS (No Signeficant) $P > 0.05$, n=9 (between 10/90 and control)).

The LDH absorbance was highest in the case of PLA, suggesting this was the most cytotoxic coating for HUVEC cells as compared to PDMMLA coatings. 30/70 coating had the lower LDH absorbance. Interestingly, there was no death cell after 24h of HUVEC incubation on 30/70. This

results supported the suggestion that 30/70 was the most biocompatible surface which was in agreement with the previous study of HUVEC morphology analyzed on different coatings. Thus, the observation study of HUVEC spreading and morphology were found to be correlated with the absorbance measure of LDH. Therefore, cellular behavior (viability migration, proliferation and differentiation) can be controlled by the measurement of initial cell spreading which is defined by its size and shape in a well-defined substrate anchoring zone. In the case of low spreading, the cell is round and slightly attached to the surface. This usually leaded to cell death. At medium spreading, cells are the most active in migration and proliferation. However, if the affinity between cell and substrate was very large with multiple adhesion sites associated with a very rich cytoskeleton (strong adhesion), the cells tend to return directly to the differentiation phase (*Fig. S6 in the ESI*) [36].

Indeed, the results of cell spreading demonstrated that the 10/90 polymer presented the best adhesion layer in contact with HUVECs (Fig. 9). It allowed a very good spreading behavior after 2h (spreading test). However, the cells adhered strongly and rapidly at first contact with the surface of 10/90. This strong HUVEC adhesion to the substrate caused it to tear over time (results of cell morphology and behavior) and leaded to less viability as compared to 20/80 and 30/70 (LDH test).

Moreover, 30/70 was the surface which was found the less pronounced in view of its HUVEC spreading and adhesion behaviors, and the most favorable for monocytes adhesion and HUVEC proliferation and viability over time compared to the other polymers. 20/80 is the surface with average adhesion and spreading properties. Consequently, the biological response of PDMMLAs, as a function of exposure time to HUVECs, was influenced by their chemical nature. PDMMLAs were the most biocompatible materials. In contrast, PLA was the least favorable surface as compared to PDMMLAs. It had a hydrophobic and rigid character and a worsted cellular response.

3.3. Recovered metallic stent morphology

As mentioned above, to improve the blood compatibility of stents, the used coating stent must have a smooth and homogeneous surface to significantly inhibit arterial lesions and platelet deposition with decreasing the friction between stent and arterial wall. In this work, scanning electron microscopic (SEM) was used to evaluate the surface homogeneity and roughness after coating the metallic stent with PDMMLAs copolymers. Figure 11 showed highly magnified high-resolution SEM images for expensed stents (bare stent, without polymer coating, and recovered stents with 10/90, 20/80 and 30/70 polymers). The SEM images of different PDMMLAs coating demonstrates

that the surfaces was very uniform and smooth, and there were not any cracks on stent surface. This enhances the potential of PDMMLAs as promising Drug Eluting Stent.

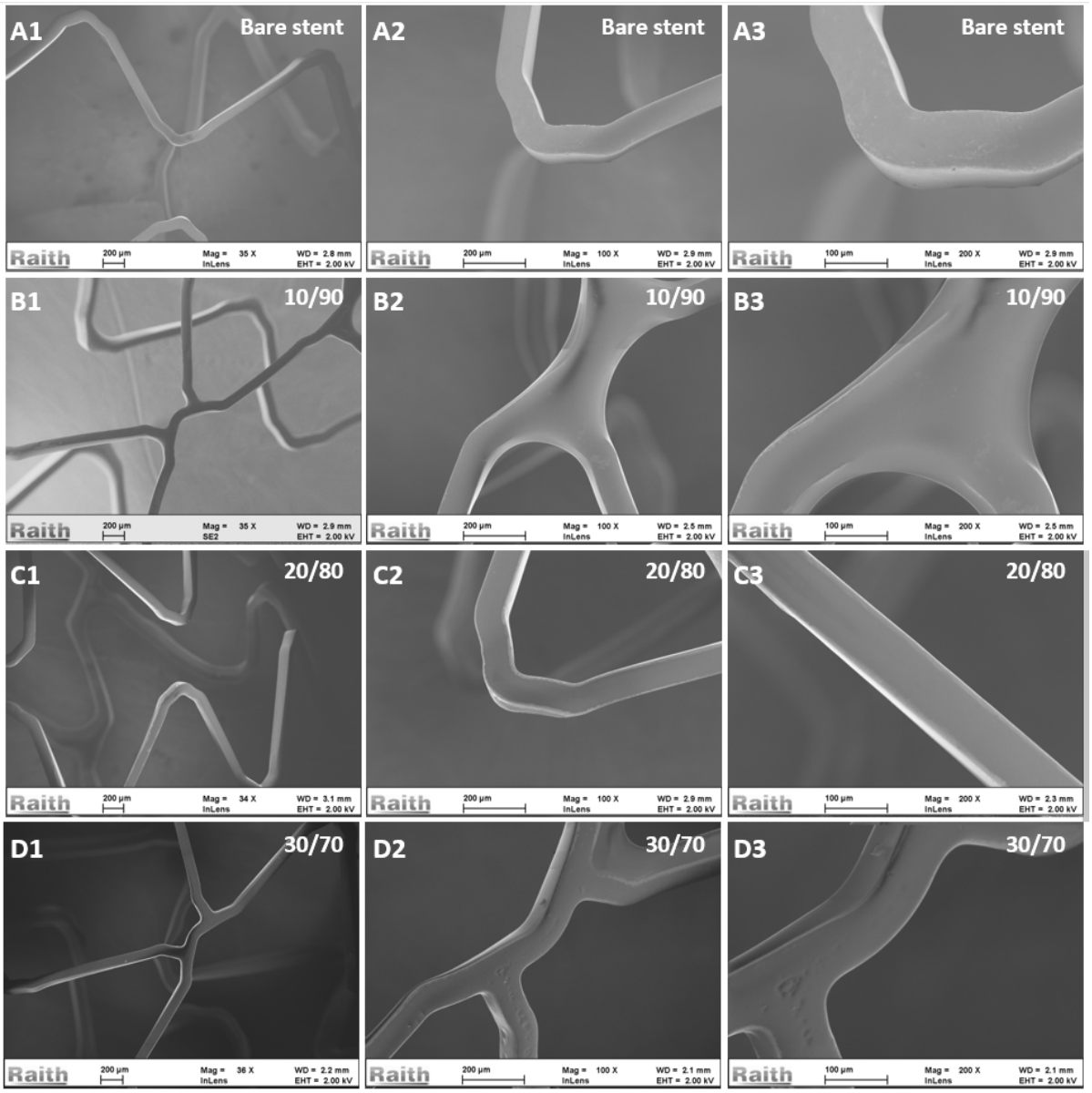

Fig. 11. SEM images of expanded stents with PDMMLAs coating (x350, x1000 and x2000 magnification): Bare stent (A1, A2 and A3), 10/90 coating (B1, B2 and B3), 20/80 coating (C1, C2 and C3) and 30/70 coating (D1, D2 and D3).

The thickness of polymer coating was estimated using the SEM microscopy. Polymer was deposited on metallic stent surface. The coating was scratched and the depth of the scratch was estimated by SEM microscopy. Indeed, the used solution of polymers to coat metallic stents gave coatings with a thin of 2 µm in thickness (Fig. 12).

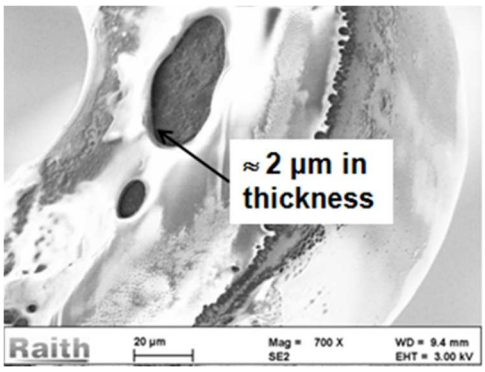

Fig. 12. SEM images of scratched 30/70 polymer coating (x5000 magnification).

4. Conclusion

This study aims to investigate the correlation between PDMMLA copolymers properties and choose the copolymer appropriate to cover metallic stent. Toward that end, PDMMLAs copolymers were selected for two objectives: chemical modifications and adjustment of the hydrophilic/hydrophobic balance, and thus the physicochemical and biological properties. Three copolymers were chosen with 10, 20 and 30% of carboxylic acid groups as potential active-coating stents because they are functionalisable, have adjustable physicochemical properties, and biodegradable. Obtained results with our copolymers were compared with those of PLA which is the most used material as stent coating. PDMMLA copolymers have good thermo-mechanical, rheological and surface properties. They have a viscoelastic behavior which favorite its use in this field contrary to PLA which has thus less ductility and softness. According to the study of HUVEC cells adhesion, spreading, morphology, behavior and proliferation and adhesion of monocytes on copolymers, we have found that PDMMLAs own good biological response which can be adjusted with their chemical modification. Finally, thanks to its better adhesion and proliferation of HUVEC cells, very favorable surface properties and rapidly degradation in physiological conditions, the amphiphilic copolymer 30/70 has been chosen as the most optimal surface to use it with a therapeutic agent.

References

[1] F. Sanchis-Gomar, C. Perez-Quilis, R. Leischik, A. Lucia, Epidemiology of coronary heart disease and acute coronary syndrome, Ann. Transl. Med. 4 (2016) 1–12.
[2] P.K. Bowen, E.R. Shearier, S. Zhao, R.J. Guillory, F. Zhao, J. Goldman, J.W. Drelich, Biodegradable metals for cardiovascular stents: from clinical concerns to recent Zn-Alloys, Adv. Healthc. Mater. 5 (2016) 1121–1140.
[3] M. Haidopoulos, S. Turgeon, C. Sarra-Bournet, G. Laroche, D. Mantovani, Development of an optimized electrochemical process for subsequent coating of 316 stainless steel for stent applications, J. Mater. Sci. Mater. Med. 17 (2006) 647–657.
[4] X.W. Ng, Y. Huang, K.L. Liu, S.G. Lim, H.H. Chen, J.C. Burnett Jr, Y.C.F. Boey, S.S. Venkatraman, In Vitro Evaluation of Cenderitide-Eluting Stent I—An Antirestenosis and Proendothelization Approach, J. Pharm. Sci. 103 (2014) 3631–3640.

[5] S. Borhani, S. Hassanajili, S.H.A. Tafti, S. Rabbani, Cardiovascular stents: overview, evolution, and next generation, Prog. Biomater. 7 (2018) 175–205.
[6] Y. Wang, P. Dong, L. Li, X. Li, H. Wang, X. Yang, S. Wang, Z. Li, X. Shang, Biodegradable polymer drug-eluting stents versus second-generation drug-eluting stents for patients with coronary artery disease: an update meta-analysis, Cardiovasc. Drugs Ther. 28 (2014) 379–385.
[7] S.K. Jaganathan, E. Supriyanto, S. Murugesan, A. Balaji, M.K. Asokan, Biomaterials in Cardiovascular Research: Applications and Clinical Implications, BioMed Res. Int. 2014 (2014) 459465. https://doi.org/10.1155/2014/459465.
[8] D.-H. Lee, J.M. de la Torre Hernandez, The newest generation of drug-eluting stents and beyond, Eur. Cardiol. Rev. 13 (2018) 54.
[9] Y. Huang, H.C.A. Ng, X.W. Ng, V. Subbu, Drug-eluting biostable and erodible stents, J. Control. Release Off. J. Control. Release Soc. 193 (2014) 188—201.
[10] J.Y. Ljubimova, J. Portilla-Arias, R. Patil, H. Ding, S. Inoue, J.L. Markman, A. Rekechenetskiy, B. Konda, P.R. Gangalum, A. Chesnokova, others, Toxicity and efficacy evaluation of multiple targeted polymalic acid conjugates for triple-negative breast cancer treatment, J. Drug Target. 21 (2013) 956–967.
[11] H. Ding, G. Helguera, J.A. Rodríguez, J. Markman, R. Luria-Pérez, P. Gangalum, J. Portilla-Arias, S. Inoue, T.R. Daniels-Wells, K. Black, others, Polymalic acid nanobioconjugate for simultaneous immunostimulation and inhibition of tumor growth in HER2/neu-positive breast cancer, J. Controlled Release. 171 (2013) 322–329.
[12] B. He, J. Bei, S. Wang, Synthesis and characterization of a functionalized biodegradable copolymer: poly (l-lactide-co-RS-β-malic acid), Polymer. 44 (2003) 989–994.
[13] B. He, J. Bei, S. Wang, Morphology and degradation of biodegradable poly (l-lactide-co-β-malic acid), Polym. Adv. Technol. 14 (2003) 645–652.
[14] B.-S. Lee, M. Vert, E. Holler, Water-soluble Aliphatic Polyesters: Poly (malic acid) s, Biopolym. Online Biol. Chem. Biotechnol. Appl. 3 (2005).
[15] B. Gasslmaier, C.M. Krell, D. Seebach, E. Holler, Synthetic substrates and inhibitors of β-poly (L-malate)-hydrolase (polymalatase), Eur. J. Biochem. 267 (2000) 5101–5105.
[16] Y. Liu, W. Wang, J. Wang, Y. Wang, Z. Yuan, S. Tang, M. Liu, H. Tang, Blood compatibility evaluation of poly (D, L-lactide-co-beta-malic acid) modified with the GRGDS sequence, Colloids Surf. B Biointerfaces. 75 (2010) 370–376.
[17] W. Wang, Y. Liu, J. Wang, X. Jia, L. Wang, Z. Yuan, S. Tang, M. Liu, H. Tang, Y. Yu, A novel copolymer poly (lactide-co-β-malic acid) with extended carboxyl arms offering better cell affinity and hemacompatibility for blood vessel engineering, Tissue Eng. Part A. 15 (2009) 65–73.
[18] J. Qian, W. Xu, W. Zhang, X. Jin, Preparation and characterization of biomorphic poly (l-lactide-co-β-malic acid) scaffolds, Mater. Lett. 124 (2014) 313–317.
[19] M. Mozafari, M. Gholipourmalekabadi, N. Chauhan, N. Jalali, S. Asgari, J. Caicedoa, A. Hamlekhan, A. Urbanska, Synthesis and characterization of nanocrystalline forsterite coated poly (l-lactide-co-β-malic acid) scaffolds for bone tissue engineering applications, Mater. Sci. Eng. C. 50 (2015) 117–123.
[20] S.L. King, V.X. Truong, C. Kirchhoefer, A. Pitto-Barry, A.P. Dove, Synthetic strategies, sustainability and biological applications of malic acid–based polymers, Green Mater. 2 (2014) 107–122.
[21] F. Ouhib, S. Randriamahefa, P. Guérin, C. Barbaud, Synthesis of new statistical and block co-polyesters by ROP of α, α, β-trisubstituted β-lactones and their characterizations, Des. Monomers Polym. 8 (2005) 25–35.
[22] V. Nurmikko, E. Salo, H. Hakola, K. Mäkinen, E.E. Snell, The bacterial degradation of pantothenic acid. II. Pantothenate hydrolase, Biochemistry. 5 (1966) 399–402.
[23] C. Goodhue, E.E. Snell, The bacterial degradation of pantothenic acid. III. Enzymatic formation of aldopantoic acid, Biochemistry. 5 (1966) 403–408.

[24] M. Lähdesmäki, P. Mäntsälä, Comparison of d-malate and β, β-dimethylmalate dehydrogenases from Pseudomonas fluorescens UK-1, Biochim. Biophys. Acta BBA-Enzymol. 613 (1980) 266–274.
[25] R. Belibel, T. Avramoglou, A. Garcia, C. Barbaud, L. Mora, Effect of chemical heterogeneity of biodegradable polymers on surface energy: A static contact angle analysis of polyester model films, Mater. Sci. Eng. C. 59 (2016) 998–1006.
[26] C. Barbaud, F. Abdillah, F. Fabienne, M. Guerrouache, P. Guérin, Synthesis of new α, α′, β-trisubstituted β-lactones as monomers for hydrolyzable polyesters, Des. Monomers Polym. 6 (2003) 353–367.
[27] F. Kohn, J. Van Den Berg, G. Van De Ridder, J. Feijen, The ring-opening polymerization of D, L-lactide in the melt initiated with tetraphenyltin, J. Appl. Polym. Sci. 29 (1984) 4265–4277.
[28] D. Cohn, H. Younes, Biodegradable PEO/PLA block copolymers, J. Biomed. Mater. Res. 22 (1988) 993–1009.
[29] I. Spiridon, K. Leluk, A.M. Resmerita, R.N. Darie, Evaluation of PLA–lignin bioplastics properties before and after accelerated weathering, Compos. Part B Eng. 69 (2015) 342–349.
[30] R. Belibel, C. Barbaud, New promising biodegradable polyesters derived from poly((R,S)-3,3-dimethylmalic acid) for biomedical applications, in: Biodegrad. Polym. Recent Dev. New Perspect., Edited by Geraldine Rohman, 2017.
[31] V. Silverajah, N.A. Ibrahim, W.M.Z.W. Yunus, H.A. Hassan, C.B. Woei, A comparative study on the mechanical, thermal and morphological characterization of poly (lactic acid)/epoxidized palm oil blend, Int. J. Mol. Sci. 13 (2012) 5878–5898.
[32] Y. Huang, Drug Eluting Stents: Anti-Inflammatory Approach To Prevent Restenosis After Stent Implantation, Leuven University Press, 2003.
[33] R. Belibel, C. Barbaud, L. Mora, Dynamic contact angle cycling homogenizes heterogeneous surfaces, Mater. Sci. Eng. C. 69 (2016) 1192–1200.
[34] R. Belibel, N. Marinval, H. Hlawaty, C. Barbaud, Poly ((R, S)-3, 3-dimethylmalic acid) derivatives as a promising cardiovascular metallic stent coating: Biodegradation and biocompatibility of the hydrolysis products in human endothelial cells, Polym. Degrad. Stab. 130 (2016) 288–299.
[35] D. Klee, H. Höcker, Polymers for biomedical applications: improvement of the interface compatibility, in: Biomed. Appl. Polym. Blends, Springer, 2000: pp. 1–57.
[36] A. Blau, Interactions between biological and non-biological devices, University of Kaiserslautern, 2005.

Graphical abstract: 531 x 1328 pixels (hxw)